

## Direct Atomic Layer Deposition of Ternary Ferrites with Various Magnetic Properties

Yuen Tung Chong,<sup>†</sup> Eric Man Yan Yau,<sup>‡</sup>  
Kornelius Nielsch,<sup>†</sup> and Julien Bachmann<sup>\*†</sup>

<sup>†</sup>Institute of Applied Physics, University of Hamburg, 20355 Hamburg, Germany, and <sup>‡</sup>Max Planck Institute of Microstructure Physics, 06120 Halle, Germany

Received September 10, 2010

Revised Manuscript Received October 5, 2010

A number of applications involving magnetic phenomena require a thin, smooth and conformal magnetic layer fabricated at low temperature, either as a film or within a more complex nanostructure: spintronics, sensing, magnetic storage, and magneto-optics. For this, atomic layer deposition (ALD) would be ideally suited. Indeed, ALD is a thin film technique in which the substrate is alternatively exposed to several gaseous reactants and a smooth conformal film is thereby deposited in layer-by-layer fashion, independently of the substrate's geometric complexity.<sup>1</sup> Despite this, no ALD reaction of ferro- or ferrimagnetic materials is available to date that simultaneously possesses the following practical advantages: (1) room-temperature ferro- or ferrimagnetism of the film without further thermal treatment, (2) air stability of the material, (3) use of commonly available precursors, and (4) fast ( $\geq 0.2$  Å/cycle) growth of smooth films.<sup>2–7</sup>

Here, we demonstrate the combination of two well-behaved binary oxide ALD processes ( $\text{Fe}_2\text{O}_3$  and either NiO or  $\text{Co}_3\text{O}_4$ ) to produce the air-stable ferrimagnetic oxides  $\text{Ni}_x\text{Fe}_{3-x}\text{O}_4$  (nickel ferrite) and  $\text{Co}_x\text{Fe}_{3-x}\text{O}_4$  (cobalt ferrite) directly using ALD. The stoichiometry and thickness of the films are highly controllable, which translates into widely tunable magnetic properties. In particular, we can obtain the stoichiometric  $\text{MFe}_2\text{O}_4$ , M = Co, Ni. Among the applications reported for  $\text{CoFe}_2\text{O}_4$  are spin valves,<sup>8</sup> multiferroic stacks,<sup>9</sup> and biomedical

ferrofluidics,<sup>10</sup> whereas  $\text{NiFe}_2\text{O}_4$  is especially suited to microwave applications.<sup>11</sup>

The homoleptic cyclopentadienyl complexes of Fe(II), Co(II), and Ni(II) (metallocenes,  $\text{Cp}_2\text{M}$ ) are combined with ozone for the ferrite ALD reactions. The metallocenes are ideal precursors for ALD—thermally stable, very volatile, reactive to oxidation (to various degrees), commercially available on large scales, and practical to handle. The  $\text{Fe}_2\text{O}_3$  ALD reactions based on ferrocene are well-documented between 200 and 500 °C and result in deposition rates varying from 0.2 to 1.4 Å per cycle.<sup>3,12</sup> The ALD process for  $\text{Co}_3\text{O}_4$  is usually carried out at slightly lower temperatures (100 to 400 °C) and results in a deposition rate of 0.5 Å per cycle.<sup>13</sup> Finally, deposition rates between 3.2 and 0.3 Å per cycle are obtained from 150 to 330 °C for nickel oxide.<sup>2,14</sup> Ozone is chosen in this work as the oxygen source in order to minimize carbon contamination and lower the deposition temperatures.<sup>3,12,15</sup> On the basis of the literature reports and our previous studies,<sup>2,3,12–14</sup> the deposition of  $\text{Co}_x\text{Fe}_{3-x}\text{O}_4$  is investigated at 250 °C and that of  $\text{Ni}_x\text{Fe}_{3-x}\text{O}_4$  at 200 °C in a Savannah reactor from Cambridge Nanotech. The samples were prepared by pulsing ferrocene and ozone, then cobaltocene (or nickelocene) and ozone, on a Si(100) substrate. One ALD supercycle consists of  $n$   $\text{Cp}_2\text{Fe}/\text{O}_3$  cycles followed by  $m$   $\text{Cp}_2\text{M}/\text{O}_3$  cycles (M = Co, Ni). This supercycle is repeated until the desired thickness is reached. The ferrocene source was heated at 100 °C, cobaltocene at 90 °C, and nickelocene at 80 °C.

The atomic ratio between cations, Fe:M, measured by energy-dispersive X-ray spectroscopy (EDX, Figure 1, open symbols) is almost directly proportional to their corresponding pulse ratios (slopes of  $\sim 0.55$  for  $\text{Co}_x\text{Fe}_{3-x}\text{O}_4$  and  $\sim 0.19$  for  $\text{Ni}_x\text{Fe}_{3-x}\text{O}_4$ ). The atomic ratio M:Fe in the deposited film is larger than the pulse ratio  $\text{Cp}_2\text{M}:\text{Cp}_2\text{Fe}$  for both M = Co and M = Ni. Additionally, the M:Fe ratio in the solid corresponding to any given  $\text{Cp}_2\text{M}:\text{Cp}_2\text{Fe}$  ratio in the gas phase is always larger for M = Ni than for M = Co. These observations are consistent with the classic reactivity trend  $\text{Ni}(\text{II}, d^8) > \text{Co}(\text{II}, d^7) > \text{Fe}(\text{II}, d^6)$  known for the metallocenes, caused by the antibonding character of the  $d$  electrons in excess of 6.<sup>16</sup> The growth rate, approximated by X-ray reflectivity (XRR) of a single thick film ( $\geq 1200$  cycles) for every

\*Corresponding author. E-mail: julien.bachmann@physik.uni-hamburg.de.

- (1) George, S. M. *Chem. Rev.* **2010**, *110*, 111.
- (2) Daub, M.; Knez, M.; Gösele, U.; Nielsch, K. *J. Appl. Phys.* **2007**, *101*.
- (3) Bachmann, J.; Escrig, J.; Pitzschel, K.; Moreno, J. M. M.; Jing, J.; Görlitz, D.; Altbir, D.; Nielsch, K. *J. Appl. Phys.* **2009**, 07B521.
- (4) Lim, B. S.; Rahtu, A.; Gordon, R. G. *Nat. Mater.* **2003**, *2*, 749.
- (5) Lee, H. B. R.; Kim, W. H.; Lee, J. W.; Kim, J. M.; Heo, K.; Hwang, I. C.; Park, Y.; Hong, S.; Kim, H. *J. Electrochem. Soc.* **2010**, *157*, D10.
- (6) Lie, M.; Klepper, K. B.; Nilsen, O.; Fjellvag, H.; Kjekshus, A. *Dalton Trans.* **2008**, 253.
- (7) Wojcik, A.; Kopalko, K.; Godlewski, M.; Guziewicz, E.; Jakiela, R.; Minikayev, R.; Paszkowicz, W. *Appl. Phys. Lett.* **2006**, *89*.
- (8) Chapline, M. G.; Wang, S. X. *Phys. Rev. B* **2006**, *74*.
- (9) Zheng, H.; et al. *Science* **2004**, *303*, 661.
- (10) Gazeau, F.; Baravian, C.; Bacri, J. C.; Perzynski, R.; Shliomis, M. I. *Phys. Rev. E* **1997**, *56*, 614.

- (11) Ozgur, U.; Alivov, Y.; Morkoc, H. *J. Mater. Sci.: Mater. Electron.* **2009**, *20*, 789.
- (12) Rooth, M.; Johansson, A.; Kukli, K.; Aarik, J.; Boman, M.; Harsta, A. *Chem. Vapor Depos.* **2008**, *14*, 67.
- (13) Donders, M. E.; Knoops, H.; Sanden, M. C. V. d.; Kessels, W. M.; Notten, P. *ECS T.* **2009**, *25*, 39.
- (14) Lu, H. L.; Scarel, G.; Wiemer, C.; Perego, M.; Spiga, S.; Fanciulli, M.; Pavia, G. *J. Electrochem. Soc.* **2008**, *155*, H807.
- (15) Lu, H. L.; Scarel, G.; Li, X. L.; Fanciulli, M. *J. Cryst. Growth* **2008**, *310*, 5464.
- (16) Crabtree, R. H. *The Organometallic Chemistry of the Transition Metals*, 2nd ed.; Wiley: New York, 1994.

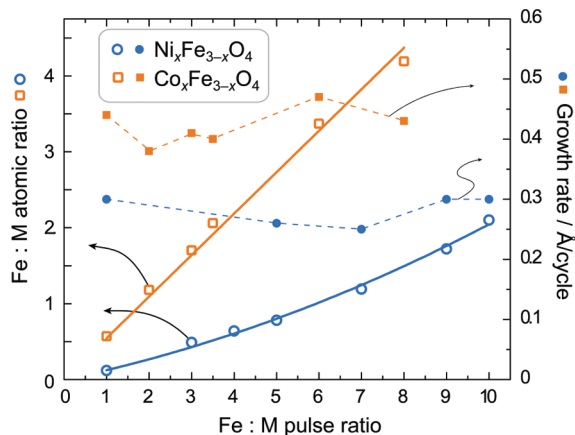


**Figure 1.** Influence of the ALD supercycle parameters on the composition and growth rate of the  $M_xFe_{3-x}O_4$  film obtained after  $\geq 1200$  ALD cycles. When a supercycle consisting of  $n$   $Cp_2Fe/O_3$  cycles and then  $m$   $Cp_2M/O_3$  cycles is repeated, the Fe:M ratio in the deposited film linearly depends on the  $n/m$  ratio, whereas the growth rate remains approximately constant. Blue,  $M = Ni$ ; orange,  $M = Co$ .

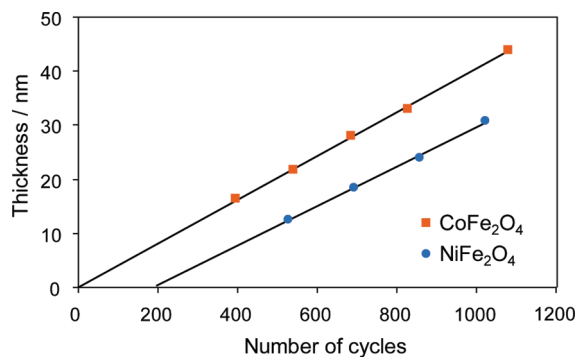


**Figure 2.** Thickness variation in stoichiometric ferrite films with the number of ALD cycles.

composition, is almost independent of the film composition,  $\sim 0.3$  Å/cycle for  $Ni_xFe_{3-x}O_4$  and  $\sim 0.4$  Å/cycle for  $Co_xFe_{3-x}O_4$ , (Figure 1, full symbols). The  $CoFe_2O_4$  thickness deposited depends linearly on the number of ALD cycles performed (Figure 2). In contrast to this, 200 cycles are required for the nucleation of a  $NiFe_2O_4$  film before the growth starts on the substrate surface. After this nucleation period, the growth is also linear, as shown in Figure 2. Atomic force microscopy (Figure 3) shows that the films deposited are smooth:  $CoFe_2O_4$  has root-mean-square (rms) roughness of 2 nm and grain size of 30 nm, while  $NiFe_2O_4$  has 0.7 and 13 nm, respectively.

$Co_xFe_{3-x}O_4$  samples with various compositions are polycrystalline and exclusively consist of the same spinel phase, as indicated by X-ray diffraction (XRD, Figure 4a). The corresponding peaks shift to lower angles when the iron concentration increases, indicating that the lattice expands: from 8.24 Å (Fe: Co = 0.58) to 8.34 Å (Fe: Co = 1.2) then 8.38 Å (Fe: Co = 1.7) and finally 8.42 Å (Fe: Co = 2), when the (311) reflection is used for calculating the lattice parameter. A similar observation

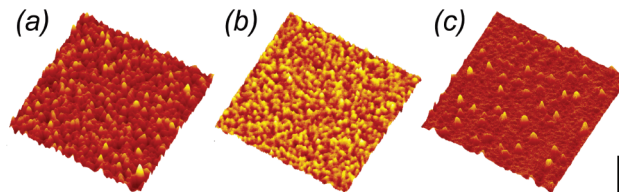


**Figure 3.** Atomic force micrographs of the film surfaces: (a)  $CoFe_2O_4$ , (b)  $NiFe_2O_4$  as deposited, and (c)  $NiFe_2O_4$  after annealing. The areas investigated are squares of (a) 1, (b) 1, and (c)  $2.5 \mu m$  size; the black vertical scale bar represents (a) 40, (b) 30, and (c) 200 nm, respectively.

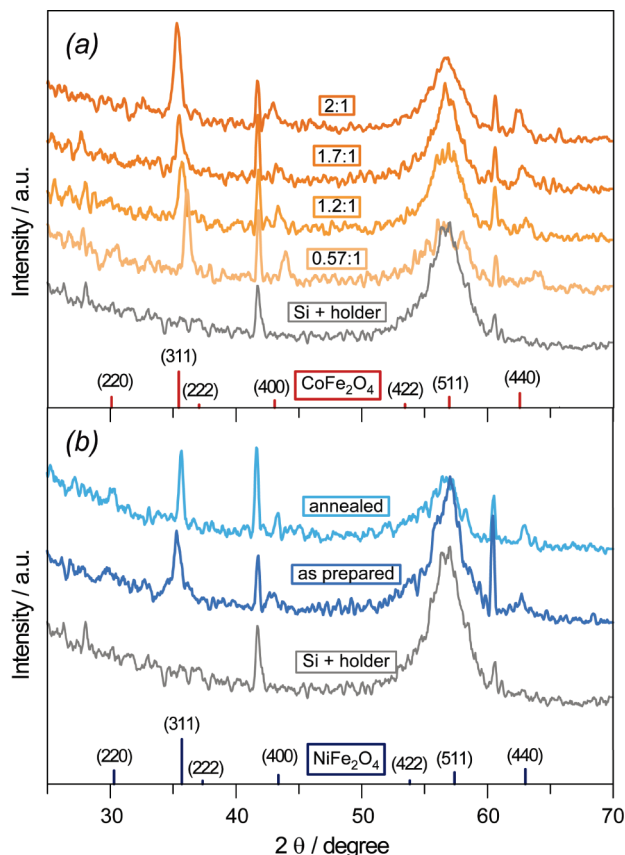


**Figure 4.** X-ray diffraction of  $M_xFe_{3-x}O_4$  thin films of various compositions. (a)  $Co_xFe_{3-x}O_4$  with stoichiometries  $1 \leq x \leq 2$ . The JCPDS reference<sup>18</sup> for  $CoFe_2O_4$  is displayed for comparison at the bottom of the graphs. (b) Diffractograms of  $NiFe_2O_4$  samples before and after thermal annealing, compared to the JCPDS reference.<sup>18</sup>

has been reported previously.<sup>17</sup> Notably, we are able to modulate the composition between the extremes  $Co_2FeO_4$  and  $CoFe_2O_4$  within the spinel phase.

The XRD reflections of most as-prepared  $Ni_xFe_{3-x}O_4$  samples are weak, revealing that the samples are only partially crystalline. As only member in the series, the  $NiFe_2O_4$  sample gives rise to stronger signals (Figure 4b). It shows a pure cubic spinel phase, with reflections slightly shifted to smaller angle compared to the JCPDS  $NiFe_2O_4$  reference.<sup>18</sup> Annealing the sample at 700 °C sharpens the XRD peaks with respect to the as-prepared sample and shifts them to the positions reported for the  $NiFe_2O_4$  standard. This is consistent with the AFM data of

(17) Bahlawane, N.; Ngamou, P. H. T.; Vannier, V.; Kottke, T.; Heberle, J.; Kohse-Hoinghaus, K. *Phys. Chem. Chem. Phys.* **2009**, *11*, 9224.

(18) JCPDS data file ( $CoFe_2O_4$ : PDF # 221086,  $NiFe_2O_4$ : PDF # 742018) International Center for Diffraction Data (ICDD).

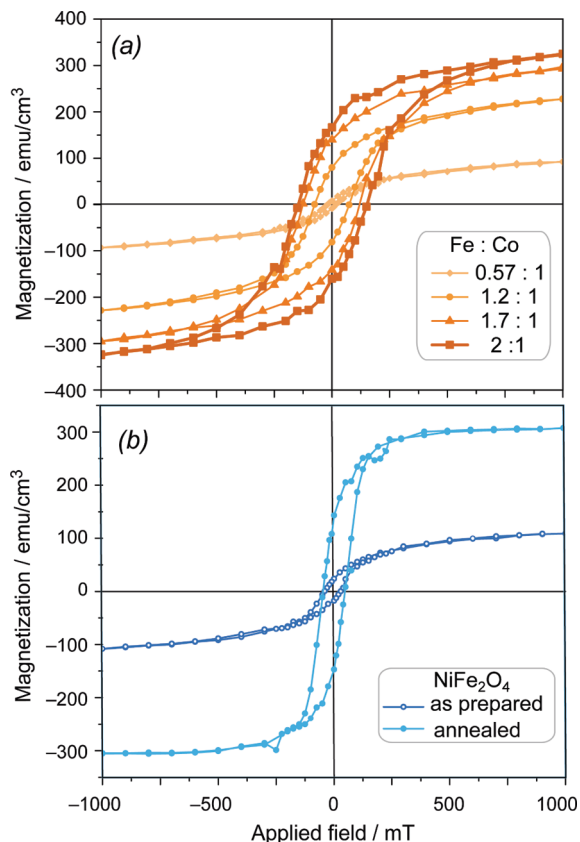


**Figure 5.** Room-temperature magnetic hysteresis loops of several ferrite films, measured in a magnetic field applied along the sample plane. (a)  $\text{Co}_x\text{Fe}_{3-x}\text{O}_4$  with stoichiometries  $1 \leq x \leq 2$ , as deposited. (b)  $\text{NiFe}_2\text{O}_4$  before and after annealing.

Figure 3c. Large crystallites have formed upon annealing of the initially smooth film under Ar for 1 h at 700 °C (rms roughness 6.3 nm).

The magnetic properties of the as-prepared Co ferrite films depend strongly on the Fe:Co atomic ratio, which also determines their crystal structure (Figure 5a). The sample of lowest Fe content has the smallest saturation magnetization ( $100 \text{ emu/cm}^3$ ) and coercive field (20 mT), corresponding to the  $\text{Co}_2\text{FeO}_4$  normal spinel. From there, both values monotonically increase upon increasing the Fe content:  $230 \text{ emu/cm}^3$  and 75 mT (Fe:Co = 1.2),  $295 \text{ emu/cm}^3$  and 122 mT (Fe:Co = 1.7), and finally  $325 \text{ emu/cm}^3$  and 150 mT for the stoichiometry  $\text{CoFe}_2\text{O}_4$ . At this point, the saturated magnetization is close to the value of bulk  $\text{CoFe}_2\text{O}_4$  ( $380 \text{ emu/cm}^3$ ).<sup>19</sup> Those values remain unchanged after storing the samples in air at room temperature for several months. The high coercive field of 150 mT is the characteristic of the hard magnetic property for which  $\text{CoFe}_2\text{O}_4$  is known. That the saturated magnetization depends on the composition is also typical in this type of ferrimagnets, since the distribution of the various metal ion types between the tetrahedral and octahedral sites of the spinel lattice strongly affects the effective magnetic moment that results in each cell from the sum

of ferromagnetic and antiferromagnetic interactions.<sup>20,21</sup> Reduced coercivity and remanence are observed for measurements carried out with the magnetic field applied perpendicular to the film surface as compared to the one parallel to the film surface (see the Supporting Information). This suggests that the preferential magnetic orientation of  $\text{CoFe}_2\text{O}_4$  is parallel to the film surface, as is the case when shape anisotropy dominates. The effect of the large magnetocrystalline anisotropy known for  $\text{CoFe}_2\text{O}_4$  is less significant because of the polycrystalline nature and small grain size of the film prepared by ALD.

In contrast to the case of  $\text{CoFe}_2\text{O}_4$ , the as-prepared  $\text{NiFe}_2\text{O}_4$  behaves as a soft magnet with a coercive field of  $\sim 35 \text{ mT}$ . Additionally, the saturation magnetization of the thin film is only  $110 \text{ emu/cm}^3$  (bulk  $280 \text{ emu/cm}^3$ ).<sup>22</sup> After annealing at 700 °C under Ar, the saturation magnetization increases to  $300 \text{ emu/cm}^3$  and the coercive field to 47 mT (Figure 5b). This corresponds to the structural improvements observed by XRD upon annealing. In a control experiment, we have observed only slight changes in the magnetism of  $\text{CoFe}_2\text{O}_4$  films after annealing.

Thus, cobalt and nickel ferrites thin films are successfully synthesized by combining ALD processes of  $\text{Fe}_2\text{O}_3$  and  $\text{Co}_3\text{O}_4$  or NiO. In each of them, the atomic ratio between the cations can be accurately tuned by controlling the pulse ratio of the corresponding precursors. All samples exhibit a single spinel phase as prepared. The  $\text{NiFe}_2\text{O}_4$  film as prepared has soft magnetic property and weak magnetic signal, further annealing is required to enhance the magnetic signal. On the contrary, stoichiometric  $\text{CoFe}_2\text{O}_4$  behaves as a hard magnet and the magnetic signal is strong, as is known for its bulk samples. The magnetic properties of  $\text{Co}_x\text{Fe}_{3-x}\text{O}_4$  samples strongly depend on their compositions.

With this, we have the possibility to deposit thin films by an ALD method that combines several advantageous properties. First, the product is magnetic at room temperature without further thermal treatment. This enables one to capitalize on one major advantage of the thin film technique ALD for applications to thermally sensitive systems, namely its low thermal budget. Second, the films deposited are air-stable, which ensures the stability of the physical properties of the sample or device upon exposure to air. Finally, the precursors are simple, commercially available molecules. Therefore, the technique should prove useful toward applications.

**Acknowledgment.** We thank Prof. A. Cebollada, Instituto de Microelectrónica de Madrid-IMM (CNM-CSIC), for performing the XRR measurements and the data analysis, as well as J. M. Montero Moreno and A. Zolotaryov (Hamburg) for their support. We acknowledge funding by the EU via the 7th framework program (project nanoMAGMA). Y.T.C. is funded by a fellowship from the DAAD.

**Supporting Information Available:** Experimental section, magnetic hysteresis curves recorded in various orientations, full ref 9 (PDF). This material is available free of charge via the Internet at <http://pubs.acs.org>.

(19) Muller, R.; Schuppel, W. *J. Magn. Magn. Mater.* **1996**, *155*, 110.

(20) Li, S. M.; Han, Z. Y.; Yang, H.; Xu, W.; Cui, Y. M.; Yu, L. X.; Feng, S. H. *J. Magn. Magn. Mater.* **2007**, *309*, 36.

(21) Pramanik, N. C.; Fujii, T.; Nakanishi, M.; Takada, J. *J. Mater. Chem.* **2004**, *14*, 3328.

(22) Smit, J.; Wijn, H. P. *Ferrites*; Philips Technical Library: Eindhoven, The Netherlands; p 157.